



ELSEVIER

Available online at www.sciencedirect.com

SCIENCE @ DIRECT®

Statistical Methodology xx (xxxx) xxx–xxx

Statistical
MethodologyOfficial Journal of the International
Indian Statistical Associationwww.elsevier.com/locate/stamet

Probabilistic modeling of percutaneous absorption for risk-based exposure assessments and transdermal drug delivery

Clifford K. Ho*

Sandia National Laboratories, P.O. Box 5800, Albuquerque, NM 87185, United States

Received 24 December 2003

Abstract

Chemical transport through human skin can play a significant role in human exposure to toxic chemicals in the workplace, as well as to chemical/biological warfare agents in the battlefield. The viability of transdermal drug delivery also relies on chemical transport processes through the skin. Models of percutaneous absorption are needed for risk-based exposure assessments and drug-delivery analyses, but previous mechanistic models have been largely deterministic. A probabilistic, transient, three-phase model of percutaneous absorption of chemicals has been developed to assess the relative importance of uncertain parameters and processes that may be important to risk-based assessments. Penetration routes through the skin that were modeled include the following: (1) intercellular diffusion through the multiphase stratum corneum; (2) aqueous-phase diffusion through sweat ducts; and (3) oil-phase diffusion through hair follicles. Uncertainty distributions were developed for the model parameters, and a Monte Carlo analysis was performed to simulate probability distributions of mass fluxes through each of the routes. Sensitivity analyses using stepwise linear regression were also performed to identify model parameters that were most important to the simulated mass fluxes at different times. This probabilistic analysis of percutaneous absorption (PAPA) method has been developed to improve risk-based exposure assessments and transdermal drug-delivery analyses, where parameters and processes can be highly uncertain.

© 2004 Elsevier B.V. All rights reserved.

Keywords: Percutaneous absorption; Exposure assessment; Transdermal; Diffusion; Probabilistic

* Tel.: +1 505 844 2384; fax: +1 505 844 7354.

E-mail address: ckho@sandia.gov.

1. Introduction

Modeling chemical transport through human skin (percutaneous absorption) serves an important role in two primary arenas: (1) hazardous chemical-exposure assessments and (2) transdermal drug delivery. In the former, models are used to understand relevant features and processes of percutaneous absorption so that protective measures can be designed and implemented that minimize the risk of dermal absorption of toxic chemicals [19,2,6,5,10,12,8,11]. In the latter arena, researchers are striving to enhance the viability of transdermal delivery of drugs such as analgesics, insulin, and more recently, peptides and proteins [1,13,7]. Transdermal delivery of drugs that require low dosages for long periods can be more effective, less costly, and less painful than traditional alternatives such as injection, intravenous infusion, or oral ingestion.

Developing accurate and reliable models of chemical transport through the skin can yield information regarding the important features and processes that contribute to the retardation or enhancement of chemical permeation. Many of the models that have been considered previously have focused on steady-state Fickian diffusion through the skin [9,6]. Transient models have been developed [16,7], but simplifying assumptions were made so that analytical solutions could be obtained. In addition, boundary conditions and properties were stylized according to the field of application (either for exposure assessment or drug delivery). For example, models used for exposure assessments typically focus on industrial solvents and other hydrocarbons (e.g., trichloroethylene), which are generally lipophilic and hydrophobic. On the other hand, models used in drug-delivery studies often focus on hydrophilic solutes (i.e., drugs that dissolve in water). These considerations impact the boundary conditions of the models, as well as the choice of partitioning coefficients and the layers of skin that are included in the models. The application-specific models make it difficult to draw general conclusions regarding the features and processes that most affect the permeability of particular solutes and solvents. In addition, models are often used with deterministic property values, which do not consider the large uncertainty inherent in biological systems and properties.

This work reviews previous models of percutaneous transport and identifies important assumptions and issues relevant to each model. A probabilistic analysis of the percutaneous absorption (PAPA) method is then developed for applications involving percutaneous exposure assessment and transdermal drug delivery. In particular, a mechanistic model of transient three-phase percutaneous absorption is developed that is used in conjunction with probabilistic methods to estimate probability distributions for permeation and chemical dose. Uncertainty distributions for model-input parameters are developed, and a Monte Carlo analysis is performed using the mechanistic model to quantify the impacts of the uncertainties on the simulated results. Sensitivity analyses are also performed to identify the parameters that are most important to the simulated results. A review of the anatomy of the skin and the factors that are likely to impact chemical permeation are provided first, followed by a description and discussion of the models and results.

2. Anatomy of the skin

The skin is a complex organ that serves to protect humans from chemical, physical, and biological intrusion, while retaining moisture and providing thermal regulation. It consists

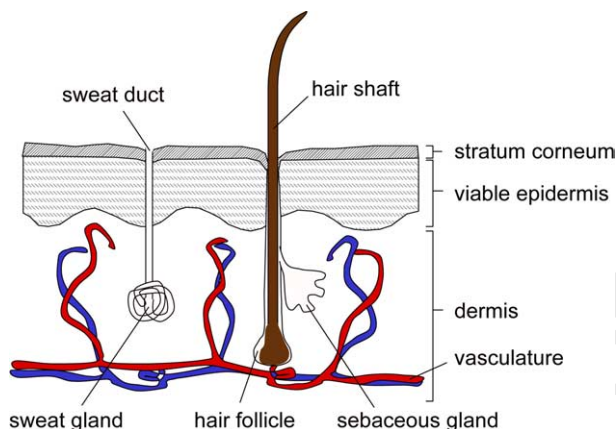


Fig. 1. Skin features relevant to percutaneous absorption of chemicals.

of three primary regions: the epidermis, the dermis, and the hypodermis (see Fig. 1). The epidermis is the outermost layer of the skin in contact with the environment, ranging between 0.075 and 0.20 mm thick in most regions and between 0.4 and 0.6 mm thick in the palms and soles [1,6]. It consists of the stratum corneum, which forms the outermost layer of the epidermis, and the viable epidermis, which consists of the granular, spinous, and basal layers. The epidermis does not contain any capillary vasculature, so chemicals that transport through the epidermis must also transport partially through the dermis to reach the bloodstream. The cells in the epidermis are continually shed to the surface and replaced from the basal layer. These cells are replaced completely on the average of once every two weeks.

The outermost layer of the epidermis, the stratum corneum, is the primary barrier to permeation of most drugs and chemicals [17,9]. The stratum corneum is between 10 and 50 μm thick (15–20 cell layers thick) and contains dead keratinized cells (keratinocytes) with lipid lamellae filling the intercellular regions. It is composed of a very heterogeneous structure containing approximately 20–40% water, 20% lipids, and 40% keratinized protein. The keratinocytes, connected together in a planar array by desmosomes, are thin platelets filled with polar protein strands woven into compact and dense keratin fibers. The lipids form a continuous, albeit extremely tortuous, intercellular network between the keratinocytes. The compactness of the keratinocytes and the limited amount of intercellular lipid results in the low permeability of the stratum corneum.

The underlying dermis contains the vasculature (blood vessels and lymph vessels) that can uptake chemicals diffusing through the skin. The vasculature can reach to within a few microns of the undersurface of the epidermis. The dermis consists of a moderately dense network of connective tissue composed of collagen fibers and elastic fibers. It varies in thickness from 1 to 4 mm depending on the location of the body. Diffusion through this layer is analogous to diffusion through hydrogels [1].

Hair follicles and sweat glands, called skin appendages, break the continuity of the epidermal and dermal layers throughout most of the surface of the body. On average,

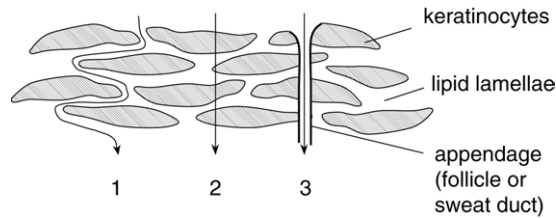


Fig. 2. Skin permeation routes: (1) intercellular diffusion through the lipid lamellae; (2) transcellular diffusion through both the keratinocytes and lipid lamellae; and (3) diffusion through appendages (hair follicles and sweat ducts).

40–100 hair follicles and 210–220 sweat ducts exist per square centimeter of skin, occupying about 0.1% of the total surface area [16]. Hair follicles extend through the epidermis into the dermis, where the base of the follicle is well vascularized. Sebaceous glands attached to the sides of the follicles secrete sebum, a lipid mixture, into the region between the hair and the sheath. The sweat glands consist of tubes extending from the dermis, where the tube is coiled and vascularized, to the skin surface where a watery mixture (sweat) is excreted to provide thermal regulation.

3. Skin permeation routes and previous models

Based on the physiology of the skin, three possible pathways exist for passive transport of chemicals through the skin to the vascular network [15,18]: (1) intercellular diffusion through the lipid lamellae; (2) transcellular diffusion through both the keratinocytes and lipid lamellae; and (3) diffusion through appendages (hair follicles and sweat ducts). Fig. 2 illustrates these potential pathways.

A number of models have been developed that simulate one or more of these pathways. Michaels et al. [9] considered the first two modes of transport by modeling the steady-state behavior of the stratum corneum as a two-phase “brick and mortar” region (the aqueous protein phase in the keratinocytes was modeled as the bricks and the intercellular lipid phase was modeled as a continuous mortar). They assumed that the transport was the sum of steady diffusion (1) through the lipid and protein in series and (2) through the lipid phase via a tortuous path. They estimated tortuosities ($\sim 10:1$) and diffusion coefficients through the lipid and protein. Experiments were conducted using cadaver skins and several different drug chemicals. Results showed a permeation dependence on pH (higher pH gave a higher flux for the same concentration) and mineral oil/water partition coefficient (larger partition coefficients yielded greater fluxes). They concluded that the ratio of the lipid diffusivity to the protein diffusivity (one of the two important parameters in their model) was 10^{-2} – 10^{-3} , meaning that the diffusion coefficient for the lipid phase was about 500 times less than the diffusion coefficient for the protein phase, which they estimated to be about $2 \times 10^{-7} \text{ cm}^2/\text{s}$ (from [9]).

Flynn [6], however, stated that the density and compactness of the intracellular protein in the keratinocytes of the stratum corneum presents a thermodynamically and kinetically impossible passageway for chemical transport. Other recent investigators also supported

the belief that when comparing evidence for intercellular versus transcellular diffusion, intercellular diffusion through the lipid lamellae is the predominant mode of transport [1]. As a result, Flynn [6] proposed an alternate “aqueous pore pathway” in parallel (as opposed to in series) with the lipid pathways through the stratum corneum to represent the limited intercellular aqueous phase. Although the locations of these aqueous pathways were uncertain, Flynn included these pathways to accommodate the diffusion of polar compounds. Other researchers have argued a similar phenomenon by considering both a polar and non-polar pathway through the stratum corneum. Elias (1981) described the polar pathway in terms of aqueous pores in the small aqueous phase between the lipid lamellae. Supporting this theory, Cooper [3] found that polar molecules such as water and small ions permeated the skin and that the flux was independent of the oil/water partition coefficient. As the polarity of the molecules decreased, the flux became a function of the partition coefficient [18].

Results of [6] showed that diffusion was a direct function of the octanol/water partition coefficient, K_{ow} , and molecular weight, MW (for a given K_{ow} , chemicals with larger molecular weights exhibited lower diffusion; for a given MW , chemicals with greater K_{ow} yielded more diffusion). The study showed that larger molecular-weight chemicals permeated slower in general, but the phase of the vehicle (water or oil) delivering the chemical was not specified. Scheuplein [17] and Potts and Guy [13] point out that the permeability of a chemical depends on the phase of the vehicle. If the molecular weight is high, indicating a more lipophilic compound, then the permeability will be greater if the vehicle is a water than an oil since the compound will want to partition out of the water and into the tissue. Flynn [6] also presented a simple exposure-assessment equation using the results of his modeling that expressed the cumulative mass entering the skin. The permeability coefficient was determined from simple equations that were correlated to experimental results for different K_{ow} and MW values. The equation assumed that the cumulative mass entering the skin took place after the lag time, which Flynn estimated could be approximately 10 min for $MW < 150$ and 1 h for $MW > 150$.

Scheuplein [16] developed analytical transient models of percutaneous absorption considering transport via appendages. He compared transport through appendages with transport through the intact stratum corneum, which he modeled as two single-phase regions: (1) the stratum corneum with a thickness of 10 μm and (2) the aqueous viable epidermis and papillary dermis with a combined thickness of 200 μm . To determine the cumulative amount of chemical transported, he used a composite slab solution (using resistances in series). From this he concluded that the appendages (follicles and sweat ducts), which had several orders of magnitude higher diffusion coefficients, allowed greater transport at early times, but that the bulk stratum corneum would allow greater diffusion at longer times. To determine concentrations profiles, he used a steady-state solution to determine the steady concentrations in the two slabs and a semi-infinite solution to determine the transient concentrations in the two slabs. The semi-infinite solution does not yield a concentration of zero at the boundary of the basal layer, which was inconsistent with his general formulation, but it did provide some relative comparisons. He also showed that the partitioning coefficient between the lipid and aqueous regions could also impact the concentration gradient.

Kalia and Guy [7] developed a number of analytical solutions for transient diffusion of drugs through the skin. They treated the skin as a homogeneous slab, but they considered different scenarios for the delivery vehicle (e.g., patch with a reservoir on top, patch with drug dispersed, drug in an ointment, etc.). They concluded that a unified model that could consider the effects of molecular weight and partition coefficients was necessary.

Other models have been developed that do not consider the specific routes of transport through the skin but attempt to describe the general rate of chemical transport through the skin and/or into the circulatory system using empirical observations and lumped-capacitance models. These models are generally described as physiologically-based pharmacokinetic models (PBPK). The general method is to correlate existing data to simple compartment models that represent the skin and various processes and regions associated with uptake into the body. Potts and Guy [13] and Poet et al. [12] have developed PBPK models that can predict chemical diffusion and uptake through the skin using physical properties of the chemical. Potts and Guy [13] developed a model that provides an algorithm to predict permeability from the drug's physical properties. Multiple regression analyses were performed using previous data of the permeability coefficient for different chemicals, and the molecular volume and the hydrogen bond activity parameters were determined to be important. However, this model is only valid when the stratum corneum is the rate-limiting barrier to percutaneous absorption (i.e., for polar compounds). Poet et al. [12] used a PBPK model to estimate skin permeability values and to predict exhaled concentrations of trichloroethylene (TCE) when subjects were exposed to TCE. Good agreement was obtained between predicted and observed TCE concentrations, but the relative importance of the various features and processes were not elucidated. In general, specific routes of permeation that contribute to the overall rate of transport through skin are not considered in PBPK models.

4. Model development

Most of the models of percutaneous absorption that have been developed previously treat the skin as a homogeneous medium with an effective (average) permeability coefficient. These include many of the transient analyses (e.g., [7]) and the PBPK analyses (e.g., [12]). A few models that do consider multiphase heterogeneous transport through the various layers and pathways of the skin often assume steady-state conditions (e.g., [9, 6]). Scheuplein [16] developed models of transient diffusion through different pathways in the skin, but deterministic models were used. In the following sections we develop a probabilistic, transient, multiphase model of chemical transport through various routes in the skin to address the inherent uncertainties in the processes and parameters associated with percutaneous absorption.

In particular, we consider the following possible pathways: (1) intercellular diffusion through the lipids and aqueous “pores” in the stratum corneum (pathway #1 in Fig. 2); and (2) diffusion through appendages (hair follicles and sweat ducts) (pathway #3 in Fig. 2). We do not consider the transcellular pathway across keratinocytes and lipids (pathway #2 in Fig. 2) because the evidence presented earlier suggests that diffusion through the keratinocytes would be extremely small.

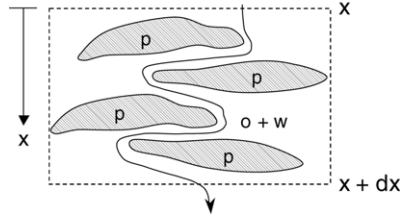


Fig. 3. Control volume for intercellular chemical diffusion through a three-phase region in the stratum corneum: p = immobile protein phase (keratinocytes), o = mobile oil (lipid) phase, w = mobile water (aqueous) phase.

4.1. Intercellular diffusion through the stratum corneum

Intercellular diffusion through the stratum corneum is modeled as a three-phase continuum. The keratinized cells in the stratum corneum are considered to be an immobile protein phase, which can provide reversible interactions (adsorption and desorption) with chemicals in the mobile phases. The mobile phases include the lipid (or oil) and aqueous (water) phases in between the keratinocytes. A differential control volume consisting of these three phases is shown in Fig. 3.

Assuming that Fick's Law governs the diffusive mass transport through the mobile regions, a one-dimensional mass balance of a chemical diffusing through this three-phase region results in the following partial differential equation for the concentration as a function of time, t [s], and penetration distance into the skin, x [m]:

$$\frac{\partial}{\partial t}(C_o\phi_o + C_w\phi_w + C_p\phi_p) = \frac{\partial}{\partial x} \left(D_o\tau_o\phi_o \frac{\partial C_o}{\partial x} + D_w\tau_w\phi_w \frac{\partial C_w}{\partial x} \right) \quad (1)$$

where C is the concentration of the chemical present in the phase [kg/m^3 -phase]; D_o , D_w , and D_p , are the molecular diffusion coefficients for the oil, water, and protein phases, respectively [m^2/s]; ϕ is the porosity of a given phase [m^3 -phase/ m^3 -total]; τ is the tortuosity coefficient (inverse of tortuosity) that expresses the ratio of the linear path length to actual path length; subscript o denotes the oil (or lipid) phase; subscript w denotes the water (or aqueous) phase; and subscript p denotes the protein (or keratinized cell) phase.

We assume that local equilibrium exists and that partitioning between the three phases can be expressed using the following linear relationships:

$$C_o = K_{ow}C_w \quad (2)$$

$$C_w = K_{wp}C_p \quad (3)$$

$$C_o = K_{op}C_p \quad (4)$$

where K is the partitioning coefficient of the phases denoted by the subscripts. Because the protein phase is hydrophilic [9], we also assume that the water–protein partition coefficient is near unity ($K_{wp} = 1$). Therefore, the water and protein concentrations are equivalent (i.e., $C_w = C_p$) and the oil–protein partition coefficient, K_{op} , is equivalent to the oil–water partition coefficient, K_{ow} (often referred to as the octanol–water partition coefficient). The octanol–water partition coefficient is used widely as a measure of polarity in organic chemistry [6]. Using these assumptions, we can then rewrite Eq. (1) in terms of the water

concentration as follows:

$$\frac{\partial C_w}{\partial t} = \frac{D_{sc}}{R_{sc}} \frac{\partial^2 C_w}{\partial x^2} \quad (5)$$

where

$$D_{sc} = D_o \tau_o \phi_o K_{ow} + D_w \tau_w \phi_w \quad (6)$$

$$R_{sc} = K_{ow} \phi_o + \phi_w + \phi_p \quad (7)$$

D_{sc} is the effective diffusion coefficient of the three-phase stratum corneum continuum and R_{sc} is the retardation factor of the three-phase stratum corneum continuum. The boundary and initial conditions for Eq. (5) are written as follows:

$$C_w(0, t) = C_w^o \quad (8)$$

$$C_w(L_{sc}, t) = 0 \quad (9)$$

$$C_w(x, 0) = 0. \quad (10)$$

Eq. (8) assumes that the surface of the stratum corneum is maintained at a constant concentration, C_w^o , in the aqueous phase. Eq. (5) assumes that at a distance L_{sc} from the surface, capillaries are present that have effectively zero concentration due to a continuous advective flow in the bloodstream (this also assumes that the aqueous region just beneath the stratum corneum in the viable epidermis and dermis does not contribute significantly to the overall resistance of chemical transport). Finally, Eq. (10) assumes that the initial concentration in the stratum corneum is zero.

The solution to Eqs. (5)–(10), which yields the aqueous concentration as a function of time and location in the skin, is presented in [4, pp. 49–51] and can be written in non-dimensional form as follows:

$$\frac{C_w}{C_w^o} = 1 - \frac{x}{L_{sc}} - \frac{2}{\pi} \sum_{n=1}^{\infty} \frac{1}{n} \sin \frac{n\pi x}{L_{sc}} e^{-\frac{D_{sc} n^2 \pi^2 t}{R_{sc} L_{sc}^2}}. \quad (11)$$

The mass flux into the blood stream (dose), \dot{m}'' [kg/m² s], can be calculated using Fick's Law at the downstream boundary of the stratum corneum (i.e., $x = L_{sc}$):

$$\dot{m}''_{sc} = -D_{sc} \left. \frac{\partial C_w}{\partial x} \right|_{x=L_{sc}} = \frac{D_{sc} C_w^o}{L_{sc}} \left(1 + 2 \sum_{n=1}^{\infty} (-1)^n e^{-\frac{D_{sc} n^2 \pi^2 t}{R_{sc} L_{sc}^2}} \right). \quad (12)$$

In addition, the cumulative amount of mass (per unit area) diffusing into the blood stream (cumulative dose), Q [kg/m²], can be expressed as follows:

$$Q_{sc} = \int_0^t \dot{m}''_{sc} dt = \frac{D_{sc} C_w^o t}{L_{sc}} - \frac{L_{sc} C_w^o R_{sc}}{6} - \frac{2 L_{sc} C_w^o R_{sc}}{\pi^2} \sum_{n=1}^{\infty} \frac{(-1)^n}{n^2} e^{-\frac{D_{sc} n^2 \pi^2 t}{R_{sc} L_{sc}^2}}. \quad (13)$$

The expressions for both the mass flux, \dot{m}''_{sc} , and cumulative dose, Q_{sc} , can be readily non-dimensionalized. Finally, the time required for the system to reach steady-state conditions,

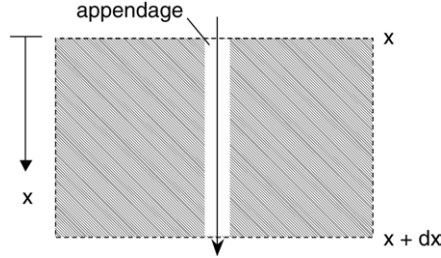


Fig. 4. Control volume for diffusion through an appendage (sweat duct or hair follicle). Diffusion is assumed to occur through a single-phase fluid in the appendage.

t_{sc}^o [s], can be approximated by the following expression adapted from [4, p. 51]:

$$t_{sc}^o \approx 0.45 \frac{L_{sc}^2 R_{sc}}{D_{sc}}. \quad (14)$$

4.2. Diffusion through sweat ducts

Chemical permeation through sweat ducts is modeled as a single-phase aqueous diffusion process. A control volume consisting of a sweat duct (or hair follicle) in a larger continuum is shown in Fig. 4. For simplicity, the region around the sweat duct is assumed to be impermeable (no interactions), and the sweat duct is assumed to be filled with water. The region around the sweat duct is included in the control volume to represent a larger unit area of skin for normalization with the other transport pathways.

A mass balance of a chemical species diffusing through this control volume can be written as follows:

$$\frac{\partial C_s}{\partial t} = \frac{D_s}{R_s} \frac{\partial^2 C_s}{\partial x^2} \quad (15)$$

where

$$D_s = D_w \tau_s \phi_s \quad (16)$$

$$R_s = \phi_s \quad (17)$$

where the subscript s denotes the sweat duct. Note that the porosity of the sweat duct, ϕ_s , represents the fractional area that the sweat ducts occupy per unit area of skin. It depends on both the density of sweat ducts and the area available for diffusion within each sweat duct. The boundary and initial conditions for Eq. (15) are the same as those expressed in Eqs. (8)–(10) with C_s replacing C_w . The constant aqueous concentration on the surface of the sweat duct is assumed to be the same as the constant aqueous concentration applied to the surface of the skin, C_w^o , in Eq. (8). In addition, the distance between the surface of the sweat duct and the location where the chemical is carried into the blood stream is denoted as L_s . The solutions for the normalized concentration, the mass flux into the bloodstream, the cumulative mass, and the time to reach steady state are expressed as

follows for chemical transport in the sweat duct:

$$\frac{C_s}{C_w^o} = 1 - \frac{x}{L_s} - \frac{2}{\pi} \sum_{n=1}^{\infty} \frac{1}{n} \sin \frac{n\pi x}{L_s} e^{-\frac{D_s n^2 \pi^2 t}{R_s L_s^2}} \quad (18)$$

$$\dot{m}_s'' = -D_s \left. \frac{\partial C_s}{\partial x} \right|_{x=L_s} = \frac{D_s C_w^o}{L_s} \left(1 + 2 \sum_{n=1}^{\infty} (-1)^n e^{-\frac{D_s n^2 \pi^2 t}{R_s L_s^2}} \right) \quad (19)$$

$$Q_s = \frac{D_s C_w^o t}{L_s} - \frac{L_s C_w^o R_s}{6} - \frac{2 L_s C_w^o R_s}{\pi^2} \sum_{n=1}^{\infty} \frac{(-1)^n}{n^2} e^{-\frac{D_s n^2 \pi^2 t}{R_s L_s^2}} \quad (20)$$

$$t_s^o \approx 0.45 \frac{L_s^2 R_s}{D_s}. \quad (21)$$

4.3. Diffusion through hair follicles

Diffusion through hair follicles is modeled in a similar fashion as diffusion through sweat ducts. The primary difference is that the follicle is assumed to be filled with an oil phase instead of an aqueous phase. Using the control volume shown in Fig. 4, a mass balance on a chemical species diffusing through the oil phase in the follicle can then be expressed as follows:

$$\frac{\partial C_f}{\partial t} = \frac{D_f}{R_f} \frac{\partial^2 C_f}{\partial x^2} \quad (22)$$

where

$$D_f = D_o \tau_f \phi_f \quad (23)$$

$$R_f = \phi_f \quad (24)$$

where the subscript f denotes the hair follicle. The porosity of the hair follicle, ϕ_f , represents the fractional area that the follicles occupy per unit area of skin. It depends on both the density of follicles and the available area for diffusion within each follicle. The boundary condition at the surface of the hair follicle is slightly different than the corresponding boundary conditions of the stratum corneum and sweat duct because the follicle concentration is written in terms of the oil phase. Assuming local equilibrium between the aqueous concentration at the surface boundary of the skin and the concentration in the oil phase at the surface of the follicle, the boundary and initial conditions for the follicle can be written as follows:

$$C_f(0, t) = K_{ow} C_w^o \quad (25)$$

$$C_f(L_f, t) = 0 \quad (26)$$

$$C_f(x, 0) = 0. \quad (27)$$

The distance between the surface of the follicle and the location where the chemical is carried into the bloodstream is denoted as L_f . The solutions for the normalized concentration, the mass flux into the bloodstream, the cumulative mass, and the time to

reach steady state are expressed as follows for chemical transport in the hair follicle:

$$\frac{C_f}{K_{ow}C_w^o} = 1 - \frac{x}{L_f} - \frac{2}{\pi} \sum_{n=1}^{\infty} \frac{1}{n} \sin \frac{n\pi x}{L_f} e^{-\frac{D_f n^2 \pi^2 t}{R_f L_f^2}} \quad (28)$$

$$\dot{m}_f'' = -D_f \frac{\partial C_f}{\partial x} \Big|_{x=L_f} = \frac{D_f K_{ow} C_w^o}{L_f} \left(1 + 2 \sum_{n=1}^{\infty} (-1)^n e^{-\frac{D_f n^2 \pi^2 t}{R_f L_f^2}} \right) \quad (29)$$

$$Q_f = \frac{D_f K_{ow} C_w^o t}{L_f} - \frac{L_f K_{ow} C_w^o R_f}{6} - \frac{2L_f K_{ow} C_w^o R_f}{\pi^2} \sum_{n=1}^{\infty} \frac{(-1)^n}{n^2} e^{-\frac{D_f n^2 \pi^2 t}{R_f L_f^2}} \quad (30)$$

$$t_f^o \approx 0.45 \frac{L_f^2 R_f}{D_f}. \quad (31)$$

It is important to note that the expressions for the mass flux into the bloodstream in the above solutions use an effective diffusion coefficient preceding the concentration gradient term. The effective diffusion coefficient accounts for the reduced area of the appendages per unit area of skin, as well as the reduced area for diffusion caused by phase interference in the three-phase stratum corneum. However, the coefficient preceding the second derivative in the diffusion equation is expressed by the *ratio* of the effective diffusion coefficient and the retardation factor, which yields the “diffusivity” for the diffusion equation that appears in the exponent term of the solutions.

4.4. Uncertainty distributions of input parameters

The parameters that are used in the solutions presented above can be highly uncertain. As a result, distributions of values were assigned to each of the input parameters using parameter values available in the literature to capture the inherent uncertainty. If insufficient data existed to define a distribution for a parameter, professional judgment was used to assign a distribution for that parameter based on the available values. For example, values of the aqueous-phase porosity in the stratum corneum were reported as 15% in [1] and 40% in [9]. Because insufficient data were available to define an appropriate distribution, a uniform distribution using these bounding values was assumed. Therefore, a number of distributions in Table 1 utilize a uniform distribution when only bounding values were available. A Monte Carlo analysis was then performed to obtain a probabilistic distribution of results using the derived solutions. Table 1 summarizes the stochastic variables and associated uncertainty distributions that were used in this study.

All of the stochastic input parameters were assumed to be independent. Although one might intuitively expect that the octanol–water partition coefficient, K_{ow} , and aqueous boundary-condition concentration (aqueous solubility), C_w^o , might be correlated, we did not assume any correlation between the input parameters (limited data from [9] support this assumption for the oil–water partition coefficient and the water solubility).

Table 1
Stochastic variables and their uncertainty distributions

Stochastic variable	Units	Distribution	Median value*	Description	References
ϕ_o	–	uniform lower bound: 0.15 upper bound: 0.20	0.18	oil-phase porosity in the stratum corneum	1
ϕ_w	–	uniform lower bound: 0.15 upper bound: 0.40	0.27	aqueous-phase porosity in the stratum corneum	1,2
ϕ_p	–	uniform lower bound: 0.35 upper bound: 0.40	0.38	protein-phase porosity in the stratum corneum	1,2
ϕ_s	–	log uniform lower bound: 3.6×10^{-5} upper bound: 8.4×10^{-3}	4.5×10^{-4}	fractional area of sweat ducts per unit area of skin (sweat duct porosity)	3
ϕ_f	–	uniform lower bound: 1.5×10^{-3} upper bound: 3.8×10^{-3}	2.8×10^{-3}	fractional area of hair follicles per unit area of skin (follicle porosity)	3
τ_o	–	log uniform lower bound: 0.01 upper bound: 0.1	0.034	oil-phase tortuosity coefficient in stratum corneum	1
τ_w	–	log uniform lower bound: 0.001 upper bound: 0.01	3.1×10^{-3}	aqueous-phase tortuosity coefficient in stratum corneum	4
τ_s	–	uniform lower bound: 0.1 upper bound: 1.0	0.56	sweat duct tortuosity coefficient	N/A
τ_f	–	uniform lower bound: 0.1 upper bound: 1.0	0.52	hair follicle tortuosity coefficient	N/A
D_w	m ² /s	log uniform lower bound: 10^{-10} upper bound: 10^{-9}	3.2×10^{-10}	molecular diffusion coefficient in aqueous phase	5
D_o	m ² /s	log uniform lower bound: 10^{-11} upper bound: 10^{-10}	3.2×10^{-11}	molecular diffusion coefficient in oil phase	6
K_{ow}	–	log normal mean log(K_{ow}): 2.0 st. dev. log(K_{ow}): 1.4	8.8	octanol–water partition coefficient	7
C_w^o	kg/m ³	log uniform lower bound: 0.003 upper bound: 800	2.0	fixed aqueous concentration at the skin surface (aqueous solubility limit)	1,8

Table 1 (continued)

Stochastic variable	Units	Distribution	Median value [*]	Description	References
L_{sc}	m	log uniform lower bound: 5×10^{-6} upper bound: 6×10^{-4}	5.9×10^{-5}	thickness of the stratum corneum	9
L_s	m	uniform lower bound: 2×10^{-4} upper bound: 4×10^{-4}	3.1×10^{-4}	length of the sweat duct	1,10
L_f	m	uniform lower bound: 2×10^{-4} upper bound: 4×10^{-4}	3.1×10^{-4}	length of hair follicle	1,10

^{*}The median value is calculated from distributions generated by Mathcad[®] 7.

1[9].

2[1].

3[16].

⁴The aqueous-phase “pores” in the stratum corneum are assumed to have tortuosity-coefficient bounds that are an order of magnitude less than the oil-phase tortuosity coefficient in the stratum corneum.

⁵[14]; representative values were taken for solutes diffusing through water.

⁶The bounds for the molecular diffusion coefficient in the oil phase are assumed to be an order of magnitude less than the bounds for the aqueous phase.

⁷[6].

⁸Water solubilities of various compounds were used from [9].

⁹[18].

¹⁰The distribution is assumed to be equal to the distribution of thicknesses between the skin surface and capillary bed.

5. Results and discussion

A Monte Carlo analysis was performed using Mathcad[®] 7 to obtain a probabilistic distribution of results using the derived analytical solutions and stochastic parameters. Uncertainty distributions listed in Table 1 were generated in Mathcad[®] 7, and the corresponding median values are reported in the table. A chemical was assumed to be applied to the surface of the skin at time zero, and the transient concentration distribution and mass flux into the bloodstream were determined. Five hundred realizations were simulated to capture the uncertainty propagated by the sixteen stochastic input variables. Sensitivity analyses using more realizations revealed that 500 realizations were sufficient.

5.1. Modeling results

For brevity, only a subset of the solutions presented in the previous section are used to illustrate the probabilistic analysis. The time required to reach steady-state conditions and the mass flux for each of the penetration routes are examined in detail here. Fig. 5 shows the distribution of times required to reach steady state for each of the three permeation routes. The median times to reach steady state are 4 min, 24 min, and 48 min for diffusion through the sweat duct, stratum corneum, and hair follicle, respectively. The distributions of steady-state times for transport through the sweat duct and hair follicle each span about two orders of magnitude. The difference between the distributions of steady-state times

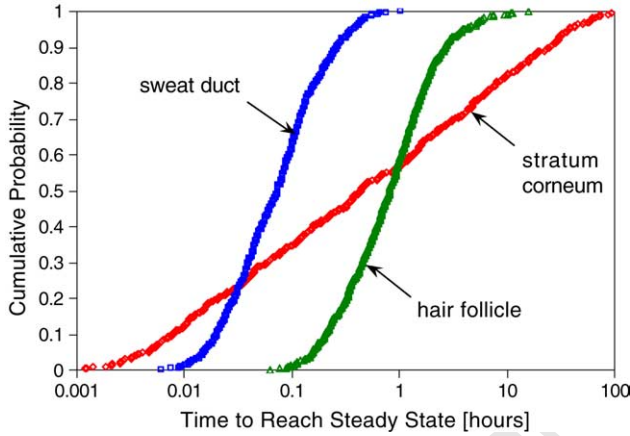


Fig. 5. Cumulative probability distribution of times required to reach steady state for chemical diffusion through three permeation routes of the skin using 500 realizations.

for the sweat duct and hair follicle is about an order of magnitude, where the sweat duct generally reaches steady state faster. The primary reason for the difference is that the molecular diffusion coefficient for the oil phase in the hair follicle was assumed to be about an order of magnitude less than the molecular diffusion coefficient for water, which comprises the sweat ducts. The results for the stratum corneum span nearly five orders of magnitude. The effective diffusion coefficient for the three-phase stratum corneum depends on a number of additional stochastic parameters that contribute additional uncertainty to the results.

The mass flux into the bloodstream for each of the three permeation routes is calculated at two different times: 60 s and 1 h. At 60 s (~ 0.02 h), Fig. 5 shows that most of the realizations for each permeation route are still in an early transient state; at 1 h, most of the realizations ($>50\%$) for each of the permeation routes have reached a steady-state condition. By evaluating the mass flux into the bloodstream at these two times, we intend to glean information regarding the most important pathways and parameters during both early-time transient diffusion as well as long-term diffusion when the pathways are approaching steady state.

Fig. 6 shows the cumulative distribution function for the mass flux into the bloodstream, \dot{m}'' , for each of the three permeation routes at 60 s. The units of mass flux used in the plot are nanograms per square centimeter per hour [$\text{ng}/\text{cm}^2 \text{ h}$] where $1 \text{ ng} = 10^{-9} \text{ g}$. At this early transient time period, many of the realizations for diffusion through the hair follicle and stratum corneum result in negligible mass flux at the lower boundary (bloodstream) of the modeled domain; however, the spread in results is significant, and values reach as high as 10^4 and $10^8 \text{ ng}/\text{cm}^2 \text{ h}$ for the hair follicle and stratum corneum, respectively. For the majority of realizations at this early time, the mass flux through the sweat duct is greatest, but the stratum corneum also plays a dominant role in nearly 40% of the realizations.

Fig. 7 shows the cumulative distribution function for the mass flux into the bloodstream, \dot{m}'' , at 1 h. At 1 h, many of the realizations have reached steady state (see Fig. 5), and

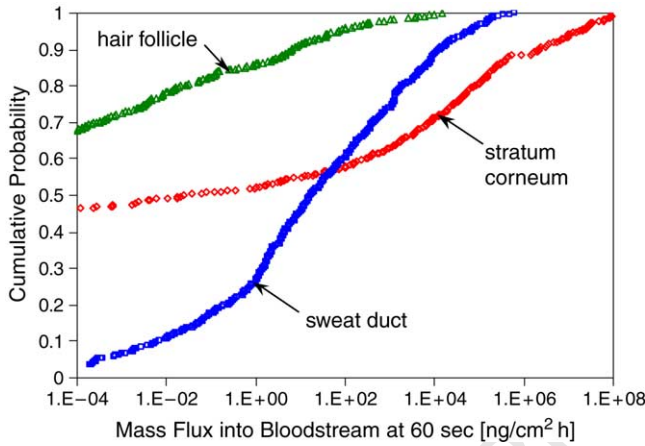


Fig. 6. Cumulative probability distribution of mass flux into the bloodstream at 60 s for chemical diffusion through three permeation routes of the skin using 500 realizations.

the spread in mass-flux values is significantly reduced for each of the three permeation routes. The distribution of results for the three-phase stratum corneum exhibits the most uncertainty, primarily because the model relies on the largest number of stochastic variables compared to the other permeation routes. In general, the mass flux into the bloodstream at 1 h is greatest in the stratum corneum, followed by the mass flux from the hair follicle and sweat duct. Recall that the mass flux into the bloodstream from the hair follicle at early times was significantly less than the mass flux from the sweat duct because of the lower molecular diffusion coefficient in the oil phase of the hair follicle. However, the fractional area of hair follicles per unit area of skin is significantly greater than the fractional area of sweat ducts (see Table 1). Therefore, after an hour (when sufficient time had elapsed for steady-state conditions to be approached), the larger fractional area of hair follicles allowed more mass to diffuse into the bloodstream per unit area of skin. Similarly, as steady-state diffusion was approached in the stratum corneum at 1 h, the large surface area allowed relatively more mass to diffuse into the bloodstream. At later times, when more of the realizations would achieve steady state in the stratum corneum, we would expect that the mass flux in the bloodstream would be dominated by the stratum corneum.

5.1.1. Comparison to empirical results

Finally, the distributions of total mass flux into the bloodstream from the three permeation routes at 60 s and 1 h are plotted in Fig. 8. The uncertainty is reduced at 1 h relative to at 60 s because as time progresses and steady-state conditions are approached, the solutions depend on fewer stochastic parameters. It is interesting to compare the resulting distributions with required dosages of various drugs reported in the literature. Amsden and Goosen [1] report that the required adult dosage for various peptides can range from 2 to 4 $\mu\text{g}/\text{day}$ for vasopressin (an antidiuretic hormone that regulates the excretion of body water through urine) to $\sim 3,000 \mu\text{g}/\text{day}$ for insulin (a hormone used to convert sugar to energy). Assuming that a transdermal patch covers approximately 10 cm^2 of skin,

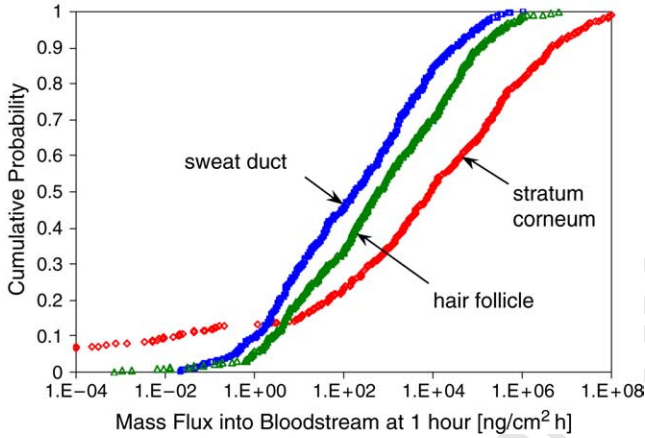


Fig. 7. Cumulative probability distribution of mass flux into the bloodstream at 1 h for chemical diffusion through three permeation routes of the skin using 500 realizations.

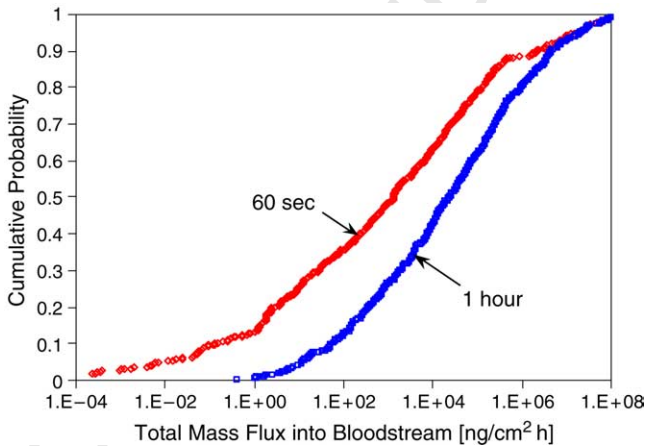


Fig. 8. Cumulative probability distribution of total mass flux into the bloodstream (sum of stratum corneum, sweat duct, and hair follicle) at 60 s and 1 h using 500 realizations.

the required average mass flux into the bloodstream would be approximately $13 \text{ ng/cm}^2 \text{ h}$ for vasopressin and $1.3 \times 10^4 \text{ ng/cm}^2 \text{ h}$ for insulin. Fig. 8 shows that the probabilities of obtaining the required mass fluxes for vasopressin and insulin at 60 s after application of the transdermal patch is about 75% and 35%, respectively, using the assumed input distributions in this model. At 1 h, the probabilities increase to 95% and 55%, respectively. It is important to note, however, that the values derived in this model are based on general input values that are intended to capture a large range of uncertainty for percutaneous absorption. Using properties specific to these two drugs (e.g., water solubility, partition coefficients, etc.) in the model will reduce the uncertainty in the results.

1
2
3
4
5
6
7
8
9

5.2. Sensitivity analyses

Analyses can be performed to determine the sensitivity of the dependent variables (e.g., mass flux into the bloodstream) to the stochastic independent variables (e.g., thickness of the stratum corneum, length of the sweat duct, etc.). A stepwise linear regression is a modified version of multiple regression that selectively adds input parameters (independent variables) to the regression model in successive steps. The stepwise process continues until no more variables with a significant effect on the dependent variable are found. The order of parameter selection for incorporation into the regression model gives an indication of their relative importance. The change in the coefficient of determination (ΔR^2) for a given step indicates the fraction of the variance in the model output explained by the input parameter added in that step.

In order to implement a linear regression, a rank transformation (assigning the smallest value of a given variable a value of 1, the next largest value of a given variable a value of 2, and so on) of independent and dependent variables is required and is generally used to compensate for potential non-linear relationships in the stepwise linear regression method for complex model results. Rank transformation essentially allows regression on the strength of the monotonic relationship, instead of the strength of the linear relationship between independent and dependent variables. This stepwise linear regression method provides insight into the relationship between uncertainty in input parameters and the uncertainty in modeling results for complex probabilistic models. In addition, this method provides a quantitative basis for prioritizing the importance of relevant input parameters and processes.

A stepwise linear-regression analysis was performed using Statistica 6.0 on the results of the total mass flux into the bloodstream at 60 s and 1 h. (Fig. 8 shows the results of the simulated total mass flux.) Table 2 lists the key parameters that were identified at 60 s and 1 h and their corresponding incremental contributions (ΔR^2) to the coefficients of determination (R^2). Also shown are the semi-partial correlations for each parameter. The semi-partial correlation is a measure of the proportion of (unique) variance accounted for by the parameter relative to the total variance of the output variable after controlling for the other input parameters. The semi-partial correlation is similar to the incremental coefficients of determination, but the sign of the semi-partial correlation indicates whether the correlation is positive or negative. Parameters with incremental coefficients of determination greater than 0.005 are presented.

At 60 s, the total mass flux is most sensitive to the aqueous solubility limit, C_w^o , which was used as the upper boundary condition for the concentration in the skin. Based on the incremental coefficient of determination, this parameter accounts for 38% of the variability in the results, with larger values resulting in larger mass fluxes. The thickness of the stratum corneum is also important, with nearly 32% of the variability in the simulated mass flux explained by this parameter. As indicated by the negative sign of the semi-partial correlation for this parameter, there is an inverse relationship between the thickness of the stratum corneum and the simulated total mass flux into the bloodstream (i.e., the thicker the stratum corneum, the lower the mass flux). The aqueous molecular diffusion coefficient and parameters associated with the sweat duct are the next most important parameters, followed by the oil-phase molecular diffusion coefficient, the octanol–water partition coefficient,

Table 2

Summary of parameters important to the simulated total mass flux into the bloodstream at two different times based on stepwise linear-regression analysis

Step	Variable	R^2	ΔR^2	Semi-partial correlation
60 s				
1	aqueous solubility limit	0.382	0.382	0.608
2	thickness of stratum corneum	0.701	0.319	−0.581
3	aqueous molecular diff. coefficient	0.727	0.026	0.172
4	sweat-duct porosity	0.751	0.024	0.151
5	sweat-duct tortuosity coefficient	0.770	0.019	0.131
6	oil molecular diffusion coefficient	0.786	0.016	0.121
7	octanol–water partition coefficient	0.800	0.014	0.113
8	oil tortuosity coefficient	0.807	0.007	0.087
1 h				
1	aqueous solubility limit	0.747	0.747	0.846
2	thickness of stratum corneum	0.875	0.128	−0.376
3	octanol–water partition coefficient	0.919	0.045	0.203
4	oil molecular diffusion coefficient	0.939	0.019	0.131
5	oil tortuosity coefficient	0.948	0.009	0.103

See Table 1 for a list of all input parameters and their distributions.

and the oil-phase tortuosity coefficient. In total, 81% of the variability in the output is explained using the multiple regression model with these eight key parameters (the top five or six parameters could be used with nearly the same confidence).

At 1 h, nearly 95% of the total variability in the simulated mass flux into the bloodstream can be explained by five key parameters. The two most important parameter are the aqueous solubility and the thickness of the stratum corneum, similar to the results at 60 s. However, the next three most important parameters are associated with transport through the oil phase in the hair follicle. As explained earlier, at 1 h, more realizations have reached steady state, and the larger number of hair follicles (follicle porosity) relative to the number of sweat ducts (sweat duct porosity) allows a greater simulated mass flux into the bloodstream when compared to earlier transient times when many of the realizations had not yet allowed mass to reach the bottom boundary.

Fig. 9 provides a graphical interpretation of the results of the stepwise linear regression using the simulated total mass flux into the bloodstream as the dependent variable. It should be noted that although the results show the strongest sensitivity to aqueous solubility limit, which was used as the aqueous-phase skin concentration at the upper boundary of the simulated domains, the distribution assigned to this parameter in Table 1 spans over five orders of magnitude. The range was taken from a variety of chemicals that were reported in the literature to capture the full uncertainty distribution for various chemicals. If the chemical of interest is prescribed or known, this parameter (or an analogous form of it, i.e., the vehicle-tissue partition coefficient per [17]) will likely exhibit a much smaller range of uncertainty. The resulting sensitivity to this parameter, while still significant, may therefore be reduced if the chemical is prescribed a priori.

Another note of interest regarding the sensitivity analysis is that the molecular diffusion coefficients for water and oil depend on a number of additional parameters

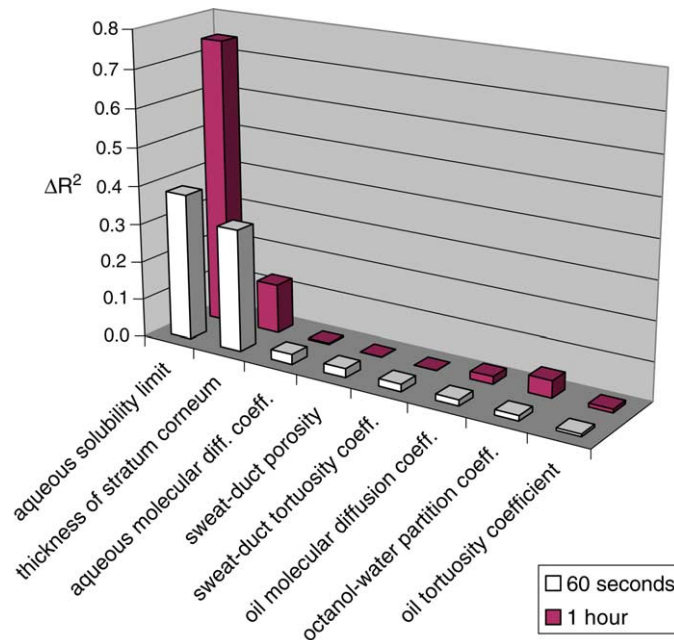


Fig. 9. Results of stepwise linear regression analysis showing the dependence of the total mass flux (sum of mass flux through stratum corneum, sweat duct, and hair follicle) on key independent stochastic parameters at two different times.

such as the molecular weight of the diffusing species, temperature, viscosity, etc. The molecular weight (or molecular volume) of a chemical has been identified as an important parameter impacting percutaneous absorption [6,13]. If a functional relationship between the molecular diffusion coefficient and these parameters had been used (see, for example, [14]), uncertainty distributions could have been assigned to these additional parameters in lieu of the diffusion coefficient to identify the relative importance of these parameters on percutaneous absorption.

5.3. Discussion

The foregoing analyses and results have illustrated significant features and benefits of a probabilistic assessment of percutaneous absorption. In particular, the ability to quantify the uncertainty associated with a specific model and to identify the parameters most important to the simulated results can benefit studies ranging from risk-based exposure assessments to transdermal drug delivery.

5.3.1. Implications for exposure assessment

The United States Environmental Protection Agency produced a comprehensive report describing the principles and applications of dermal exposure assessment [5]. The report summarizes the mechanisms of dermal absorption, techniques for measuring dermal absorption, and mathematical models available at the time for dermal absorption and

risk assessment. The purpose of this report was to provide exposure assessors with the knowledge and tools required to evaluate dose and subsequent health risks associated with dermal exposure at waste disposal sites or contaminated soils where contaminants could reside in soil, air, and water. The report stated that exposure and risk assessment associated with dermal contact remains the least well understood of the major exposure routes (relative to ingestion and inhalation) because considerable uncertainty exists in the parameters and processes associated with dermal absorption. Strangely, all of the mechanistic models presented in the report are deterministic in nature; none of them provide a quantification of uncertainty or sensitivity analyses of the mechanisms and parameters associated with percutaneous absorption. We believe that the use of probabilistic analyses that incorporate inherent uncertainty in the model parameters and processes will yield more useful and meaningful results when determining and reporting health risks associated with dermal absorption.

5.3.2. Implications for transdermal drug delivery

One of the significant problems of transdermal drug delivery is the ability to deliver sufficient doses of a particular drug through the skin. Several methods have been developed to augment the passive diffusion of water-soluble drugs such as peptides and proteins through the skin [1], and these are briefly summarized below:

- *Prodrugs*: Lipophilic groups are covalently bonded onto functional groups of the drug to improve partitioning into the intercellular lipid lamellae of the stratum corneum. Enzymes detach the lipophilic groups in vivo, rendering them free and active. However, prodrugs have molecular size restrictions and require synthesis.
- *Chemical permeation enhancers*: Compounds exist that alter the skin as a permeability barrier. Known permeation enhancers include solvents and surfactants; however, the physical basis for the method of enhancement is still unknown. No general theory of chemical enhancement has been provided.
- *Iontophoresis*: An iontophoretic device consists of two electrodes immersed in an electrolyte solution and placed on the skin. When an electric current is applied across the electrodes, an electric field is created across the stratum corneum that drives the delivery of ionized drugs. The primary route of ion transport appears to be through hair follicles or sweat glands, although additional uncertain pathways may be created. This method is restricted to short-term delivery.
- *Electroporation*: Electroporation involves the application of high-voltage electric pulses to increase the permeation through lipid bilayers. This differs from iontophoresis in the duration and intensity of the application of electrical current (iontophoresis uses a relatively constant low-voltage electric field). The high-voltage electric pulse of electroporation is believed to induce a reversible formation of hydrophilic pores in the lipid lamellae membranes that can provide a high degree of permeation enhancement, but the physics and dynamics of this process are not completely understood. This method is restricted to short-term delivery.
- *Ultrasound*: Ultrasound applies sound waves having a frequency greater than 16 kHz to the skin, which causes compression and expansion of the tissue through which the sound waves travel. The resulting pressure variations cause a number of processes (e.g., cavitation, mixing, increase in temperature) that may increase the permeation of drugs.

Again, the exact processes and physics have not yet been determined, and this method is restricted to short-term delivery.

In all of these methods, significant uncertainty exists regarding the processes and parameters that truly cause enhanced permeation. Probabilistic simulations and sensitivity analyses coupled with mechanistic models of each of these processes can help to identify the most likely processes and parameters that are significant to drug-delivery enhancement.

Finally, an additional uncertainty that has not been explicitly discussed in this paper is the potential for the chemical at the skin surface to exist as a mixture of different substances. Solubility, partitioning coefficients, and transport characteristics of the bulk fluid can vary depending on the composition of the chemical mixture. Because this analysis has evaluated parameter uncertainty by including a wide range of chemicals, the relative importance of individual parameters identified in this study should still be valid if the bulk properties of the chemical mixture are within the range of the property distributions used in this study. More rigorous analyses could be conducted by developing specific parameter distributions for specific chemicals or mixtures of chemicals and conducting a similar probabilistic analysis as described in this paper.

6. Conclusions

Percutaneous absorption plays an important role in applications dealing with exposure assessment and transdermal drug delivery. Unfortunately, previous models have focused on deterministic, steady-state, homogeneous systems when evaluating chemical transport through the skin. In this study, a probabilistic, transient, three-phase model of percutaneous absorption has been developed to assess the relative importance of uncertain parameters and processes. Penetration routes through the skin that were modeled include the following: (1) intercellular diffusion through the stratum corneum comprised of an immobile protein phase, a mobile aqueous (water) phase, and a mobile oil (lipid) phase; (2) aqueous-phase diffusion through sweat ducts; and (3) oil-phase diffusion through hair follicles. Uncertainty distributions were assigned to model parameters and a probabilistic Monte Carlo analysis was performed to simulate a distribution of mass fluxes through each of the routes. Results indicated that at early times, before steady-state conditions had been established, transport through the sweat ducts provided a significant amount of mass flux into the bloodstream. Because of the uncertainty in the input parameters, a large range of mass fluxes were simulated through each of the three routes at this early time. At longer times (1 h), when many of the realizations had reached steady state, the uncertainty was reduced, and the relative importance of the pathways had changed. Diffusion through the stratum corneum became important because of the relatively large surface area. Similarly, despite the lower oil-phase molecular diffusion coefficient of the hair follicles, diffusion through the hair follicles was more significant than diffusion through the sweat ducts at later times because of the larger simulated porosity of hair follicles.

Sensitivity analyses were also performed using a stepwise linear-regression analysis. Parameters that were most important to the simulated mass flux were identified, and the relative importance of each parameter was quantified through the incremental coefficients of determination and semi-partial correlations (see Table 2). These analyses

were found to be extremely useful in not only quantifying the uncertainty in the simulated output variables, but also identifying the input parameters that were most important to the simulated results. These probabilistic methods can provide more meaningful interpretations of exposure assessments and risk regarding dermal uptake of contaminants. In addition, new methods of enhancing transdermal drug delivery (e.g., ultrasound, electroporation, etc.) have a great deal of uncertainty surrounding the physical processes associated with these methods. Mechanistic models of multiphase, heterogeneous transport through the skin coupled with probabilistic analysis can shed additional insight into how these methods can be improved through identification and refinement of important parameters and processes.

Acknowledgments

This work was supported by Sandia's Laboratory Directed Research and Development (LDRD) project 38723/1.3. Sandia is a multiprogram laboratory operated by Sandia Corporation, a Lockheed Martin Company for the United States Department of Energy's National Nuclear Security Administration under contract DE-AC04-94AL85000.

References

- [1] B.G. Amsden, M.F.A. Goosen, Transdermal delivery of peptide and protein drugs: an overview, *AIChE Journal* 41 (8) (1995) 1972–1997.
- [2] M.G. Bird, Industrial solvents: some factors affecting their passage into and through the skin, *Annals of Occupational Hygiene* 24 (2) (1981) 235–244.
- [3] R.R. Cooper, Increased skin permeability for lipophilic molecules, *Journal of Pharmaceutical Sciences* 73 (1984) 1153.
- [4] J. Crank, *The Mathematics of Diffusion*, 2nd edition, Oxford University Press, Oxford, 1975.
- [5] Environmental Protection Agency (EPA), Dermal exposure assessment: principals and applications, Report EPA/600/8-91/011B, U.S. Environmental Protection Agency, Washington, DC, 1992.
- [6] G.L. Flynn, Physicochemical determinants of skin absorption, in: *Proceedings of the Workshop on Principles of Route-to-Route Extrapolation for Risk Assessment*, Hilton Head, SC, March 19–21, Elsevier, 1990, pp. 93–127.
- [7] Y.N. Kalia, R.H. Guy, Modeling transdermal drug release, *Advanced Drug Delivery Reviews* 48 (2001) 159–172.
- [8] J.N. McDougal, M.F. Boeniger, Methods for assessing risks of dermal exposures in the workplace, *Critical Reviews in Toxicology* 32 (4) (2002) 291–327.
- [9] A.S. Michaels, S.K. Chandrasekaran, J.E. Shaw, Drug permeation through human skin: theory and in vitro experimental measurement, *AIChE Journal* 21 (5) (1975) 985–1996.
- [10] S.A. Ness, *Surface and Dermal Monitoring for Toxic Exposures*, Van Nostrand Reinhold International Thomson Publishing Company, New York, 1994.
- [11] T.S. Poet, J.N. McDougal, Skin absorption and human risk assessment, *Chemico-Biological Interactions* 140 (2002) 19–34.
- [12] T.S. Poet, R.A. Corley, K.D. Thrall, J.A. Edwards, H. Tanojo, K.K. Weitz, X. Hui, H.I. Maibach, R.C. Wester, Assessment of the percutaneous absorption of trichloroethylene in rats and humans using MS/MS real-time breath analysis and physiologically based pharmacokinetic modeling, *Toxicological Sciences* 56 (2000) 61–72.
- [13] R.O. Potts, R.H. Guy, A predictive algorithm for skin permeability: the effects of molecular size and hydrogen bond activity, *Pharmaceutical Research* 12 (11) (1995) 1628–1633.
- [14] R.C. Reid, J.M. Prausnitz, B.E. Poling, *The properties of gases and liquids*, 4th edition, McGraw Hill, Inc., New York, 1987.

- 1 [15] R.J. Scheuplein, Mechanism of percutaneous absorption I. Routes of penetration and the influence of
2 solubility, *Journal of Investigative Dermatology* 45 (5) (1965) 334–346.
- 3 [16] R.J. Scheuplein, Mechanism of percutaneous absorption II. Transient diffusion and the relative importance
4 of various routes of skin penetration, *Journal of Investigative Dermatology* 48 (1) (1967) 79–88.
- 5 [17] R.J. Scheuplein, Percutaneous absorption after twenty-five years: or “old wine in new wineskins”, *Journal*
6 *of Investigative Dermatology* 61 (1976) 31–38.
- 7 [18] R.J. Scheuplein, I.H. Blank, Permeability of the skin, *Physiological Reviews* 51 (1971) 702–747.
- 8 [19] R.D. Stewart, H.C. Dodd, Absorption of carbon tetrachloride, trichloroethylene, tetrachloroethylene,
9 methylene chloride, and 1,1,1-trichloroethane through the human skin, *AIHA Journal* 25 (5) (1964)
10 439–446.